Laser and Particle Beams (2002), *20*, 521–526. Printed in the USA.

DOI: 10.1017/S026303460210.1017/S0263034602202281

Experimental investigations of multiple weak shock waves induced by intense heavy ion beams in solid matter

C. CONSTANTIN,[1] E. DEWALD,[1] C. NIEMANN,[1] N.A. TAHIR,[1] A. SHUTOV,[2] A. KOZYREVA,[1] T. SCHLEGEL,[1] S. UDREA,[1] D. VARENTSOV,[1] J. JACOBY,[3] A. TAUSCHWITZ,[1] U.N. FUNK,[1] U. NEUNER,[3] P. SPILLER,[3] AND D.H.H HOFFMANN[1,3]

[1]Technische Universitaet Darmstadt, Institut fuer Kernphysik, 9, 64289 Darmstadt, Germany
[2]Institute of Chemical Physics, Russian Academy of Science in Chernogolovka, Chernogolovka, 142432 Moscow Region, Russia
[3]Gesellschaft fuer Schwerionenforschung Darmstadt mbH, 64291 Darmstadt, Germany

(RECEIVED 1 March 2002; ACCEPTED 8 April 2002)

Abstract

The dynamics of low entropy weak shock waves induced by heavy ion beams in solid targets was investigated by means of a schlieren technique. The targets consist of a metallic absorber for the beam energy deposition followed by a plexiglass block for optical observations. Multiple waves propagating with supersonic velocities at 15 kbar pressures were observed in the plexiglass, for pressures of up to 70 kbar numerically calculated in the absorbers. Pressures in the megabar ranges are predicted for a near future beam upgrade, enabling studies of phase transition to metallic states of H, Kr, and Xe.

Keywords: Cold compression; Equation of state; Heavy ion beam; Weak shock waves

1. INTRODUCTION

The shock wave compression of solid matter is an issue of close relevance to the equation-of-state (EOS) studies, with applications to the phase transition to high conductive states of matter (Wigner & Huntington, 1935; Aoki & Meyer-ter-Vehn, 1994; Mao & Hemley, 1994; Weir *et al.*, 1996; Tahir *et al.*, 2001) and astrophysics. Typical approaches are the single shock and the multiple shock waves compression techniques. The former method is a fast process which follows a Hugoniot curve in the (p,V) phase space (Fig. 1, T4 Group, 1983), leading at high pressures to maximum densities of four to six times the solid state density in planar geometries. Experiments with intense lasers showed a six-fold compression (Da Silva *et al.*, 1997; Collins *et al.*, 1998) obtained with a single shock wave generated by the ablation pressure, giving rise to steep temperature, density, and pressure gradients. A uniform, cold compression is preferable, especially when a clear distinction between a state of high conductivity as a plasma and a metallic state has to be made. Compression at low temperatures can be achieved with multiple shock waves (Aoki & Meyer-ter-Vehn, 1994; Weir *et al.*, 1996), for which a heavy ion beam is a suitable driver. By means of a slowly driven reverberating shock wave, density ratios up to 10 or more can be attained (Schlegel *et al.*, 2001). The process is governed by the amount of specific energy deposited homogeneously in the target, culminating in the Bragg peak region where the entire beam is stopped. The present synchrotron (SIS) at Gesellschaft fuer Schwerionenforschung (GSI) can deliver beams with up to 10^{11} particles per bunch, 300-MeV/nucleon energies, and 300-ns pulse durations. At these parameters, strongly coupled plas-

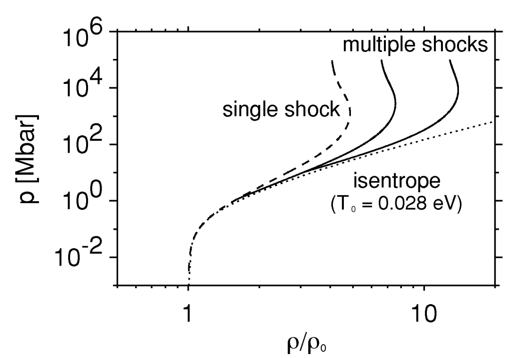

Fig. 1. Hugoniot curves showing single and multiple shocks in aluminum, calculated with the SESAME equation-of-state data.

Address correspondence and reprint requests to: Carmen Constantin, Plasma Physics Group, GSI Darmstadt, Planckstrasse 1, 64291 Darmstadt, Germany. E-mail: C.Constantin@gsi.de

mas of some cubic millimeter volume are created at solid state density and temperatures below 1 eV (Funk *et al.*, 1998; Stöwe *et al.*, 1998). At a specific energy deposition of up to 4 kJ/g, which is achieved by a plasma lens fine focusing (Stetter *et al.*, 1993, 1996), the heated matter in the Bragg region represents a source of stress waves propagating in the surrounding material (Tahir *et al.*, 1999). An insight into the behavior of the solid target under the action of these stress waves was the subject of a series of measurements aiming at the determination of pressures, densities, and stress wave propagation velocities in cold matter. This is an important first step in the context of a near future beam intensity and short bunching upgrade which will yield pressures in the megabar range (Tahir *et al.*, 2000) and thus enable experiments on phase transition toward the metallic state in solid crystals of hydrogen and noble gases.

2. EXPERIMENTAL SETUP

The first time-resolved experimental investigation of heavy-ion-driven weak shock waves inside a solid target are reported here. The experiment employed a schlieren technique assisted by a two-dimensional hydrodynamic code for simulations. With the schlieren method, an accurate dynamical visualization of the pressure waves traversing a transparent medium can be achieved. Estimations of density gradients in the target and measurements of the propagation velocities are possible. The technique relies on the detection of transmitted light that is deflected due to changes in the index of refraction in the sample material. These changes are associated with density gradients induced by the pressure waves in the target. As light source, a cw He-Ne laser with 5 mW power at 632.8 nm wavelength expanded to a parallel beam of 30 mm diameter was used (Fig. 2). The laser beam was focused by a 1000-mm focal length lens onto a beam stop which was a cylindrical wire of a diameter varying between 0.8 mm and 1.6 mm placed perpendicularly to the expected light deflections. In this experiment, a time-resolved detection with a 150-ns resolution was achieved by a streak camera (Hamamatsu C2830). Together with a fast shutter camera (PCO DICAM PRO) for 2D visualizations of the shock front, the streak camera was focused onto the target to gain space resolution. The expanded parallel laser beam probed the target perpendicular to the direction of the heavy ion beam. The target design was determined by the condition of accomplishing cold compression with the heavy ion beam and by the optical diagnostic requirements for a transparent medium. Different multilayered targets composed from a beam energy absorber made of Al, Cu, Fe, or Pb followed by a plexiglass block and an Al confiner were used. The targets were placed at the position of the ion beam focus, which had a FWHM diameter of 0.7 mm, in order to enhance the specific energy deposition.

In this single-shot experiment, a $^{83}Kr^{36+}$ ion beam with a particle energy of 300 MeV/nucleon, $2 \cdot 10^{10}$ particles/pulse, and a pulse duration of 700 ns was employed. To

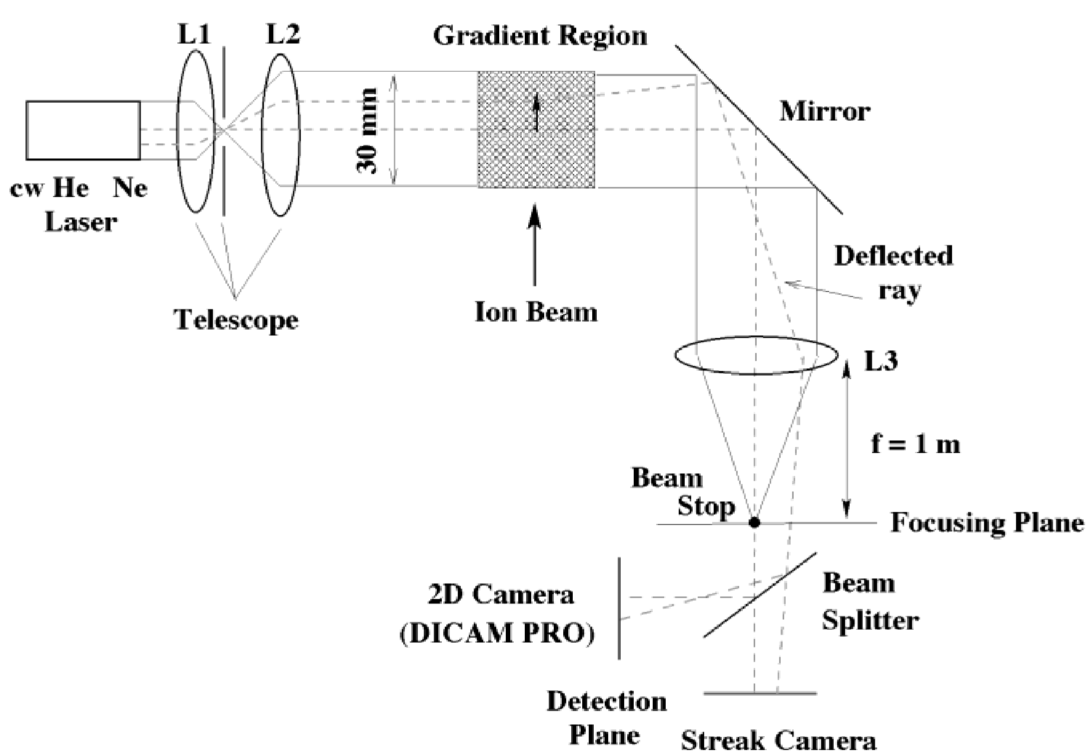

Fig. 2. Experimental schlieren setup.

https://doi.org/10.1017/S0263034602202281 Published online by Cambridge University Press

achieve cold compression of the plexiglass, it is absolutely essential to avoid penetration of the projectile particles into the plexiglass layer. Therefore, the length of the absorber was chosen to be 1 mm longer than the stopping range of the ions. According to numerical simulations, such beam intensities can heat material to a few thousand Kelvin, and therefore the stopping data in negligibly ionized matter provided by the TRIM code (Ziegler *et al.*, 1996) could be used.

A measure of the gradients induced by the shock waves in the plexiglass layer is given by the angles under which the laser rays are deflected in the perturbed region. The angular displacement can be expressed, for a one-dimensional density gradient along the ion beam axis z, as

$$\alpha = \int_{y_1}^{y_2} \frac{1}{n} \frac{\partial n}{\partial z} dy, \quad (1)$$

where α is the angular displacement in radians, n is the index of refraction, and $y_{1,2}$ is the target limits on the laser path (Jahoda & Sawyer, 1971). In the case of spherical shocks, this relation is valid only for rays crossing the target on the ion beam axis. Therefore the slit of the streak camera was always aligned to the beam axis. A further correlation between the index of refraction and mass density is given by the Clausius–Mosotti relation for fluids (Marton & Marton, 1981), under the consideration that plexiglass is a viscoelastic fluid:

$$\frac{n^2 - 1}{n^2 + 2} = K(\lambda) \cdot \rho, \quad (2)$$

where $K(\lambda)$ is an empirical constant which depends on the laser wavelength and on the material.

3. EXPERIMENTAL RESULTS

The experimental streak pictures (Fig. 3) give the amount of the deflected laser light which can be related to the deflection angles using an off-line *in situ* schlieren calibration. The deflection of the light was simulated by displacing the beam stop away from the laser focal spot, perpendicular to the laser direction. For each position, the intensity in the recorded streak picture was measured, starting from the optical noise level. Using $d = f \cdot \alpha$ where d is the displacement from the focus and f is the focal length of the lens, a relation between intensity of the deflected light and α could be obtained. By using beam stops with sizes between 0.8 mm and 1.6 mm, recordings of the longitudinal shocks travelling through the plexiglass on the beam axis were taken, revealing angular displacements larger than 0.8 mrad. They were calculated by using equation $d = f \cdot \alpha$ and compared with the values given by the calibration curve of the setup described above. The propagation velocities of the shocks were determined directly from the streak pictures with an accuracy of ± 0.1 km/s (see Table 1). Their values are slightly higher than

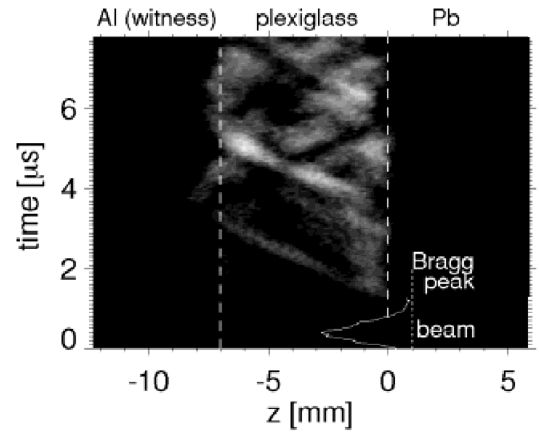

Fig. 3. Streak picture of a Pb-plexiglass-Al target. The 700-ns beam pulse comes from the right side and its temporal profile is plotted at the location of the Bragg peak. The plexiglass region is indicated by the white, dashed lines.

the speed of sound in plexiglass, which is 2.6 km/s according to the EOS data at room temperature from Lomonosov *et al.* (1994). The pressures exerted in the plexiglass were estimated using empirical data from literature (Zhang & Müller, 1984), obtained for the same pressure and velocity ranges in plexiglass as shown in Table 1. An interesting feature of the stress wave behavior is the multiple shock structure displayed in the schlieren pictures (Fig. 3), starting around 0.7 μs after the beam is stopped in the driver. The time intervals between the secondary waves emerging from the interface between absorber and plexiglass show a dependence on the material. For Al and Fe, these time intervals are smaller than for Cu and Pb. Possible explanations for the origin of the multiple waves and their time history are related to the state of the matter in the Bragg peak region, which was around 1 mm apart from the boundary with the plexiglass block. The deposited energy heats the material and changes its characteristics by bringing it above the melting point. Successive reflections will occur on the created interface between the fluid state of the matter in the Bragg peak region and the rest of the cold material, as observed also in other experiments using light ions (Baumung *et al.*, 1996). The

Table 1. *The measured parameters in plexiglass, for targets with different absorber materials.*

Absorber	v_{plexi} (km/s)	P_{plexi} (kbar)
Al	3.50	>14.9
Fe	3.20	11.9
Cu	2.88	3.0
Pb	3.00	3.7

https://doi.org/10.1017/S0263034602202281 Published online by Cambridge University Press

Bragg region is more spatially restricted in the case of Al and Fe than for the other two metals where the maximum temperatures reached were higher. A wave reflected from this interface propagates with smaller acoustic velocity in Cu (3.95 km/s) and Pb (1.91 km/s) than in Al (5.2 km/s) and Fe (5.7 km/s). The consequent effect is reflected in the time intervals between the multiple waves' arrival, which were smaller for Al and Fe than for Cu and Pb. These premises were confirmed by simulations carried out with a one-dimensional hydrodynamic code—MULTI 1D—which clearly showed the weak multiple shocks in both regions of interest—the plexiglass and the nonheated metallic pusher in front of the Bragg peak region. Both in simulation and experiment, the second wave showed an increased velocity related to the first wave velocity. This fact is explained by a pressure enhancement, since the second wave propagates through a material already compressed by the first shock.

4. NUMERICAL CALCULATIONS AND COMPARISON WITH THE EXPERIMENT

The experimental data was compared with the results of a two-dimensional hydrodynamic code, BIG2, that treats interfaces with the Godunov method in moving grids (Fortov *et al.*, 1996). A semi-empirical wide range EOS (Bushmann & Fortov, 1987; Lomonosov *et al.*, 1994) was used and the input beam parameters, as well as the target geometry were complying with the experimental conditions. Benchmarks such as the shock velocity in plexiglass and the velocity of the expanding matter in front of the target, measured by backlighting shadowgraphy, were provided by the experiment. The calculated parameters are given in Table 2, showing a good agreement for the targets with Cu and Pb absorbents, and less agreement for Fe.

For a direct comparison with the experiment, the temporal density profiles for plexiglass (Fig. 4) were used, together with relations (1) and (2), to rebuild the streak pictures as given by the schlieren technique (Fig. 5). The comparison between the experimental and the simulated pictures outlines the good agreement in the wave propagation velocities and the delays of the secondary waves. According to the simulations, the maximum pressure induced by the heavy ion beam in the metallic absorbers was 70 kbar in the Bragg peak. The resulting compression factor in plexiglass, for these ion beam parameters, was 1.10 (for the target with Pb absorber), at a temperature increase of only 4 K.

Table 2. *The calculated parameters in plexiglass and absorbents for three layered targets, using the BIG2 code.*

Absorber	v_{plexi} (km/s)	P_{plexi} (kbar)	T_{metal} (K)	P_{metal} (kbar)
Fe	2.70	1.5	2900	30
Cu	2.80	2.1	3468	35
Pb	2.87	4.5	7380	71

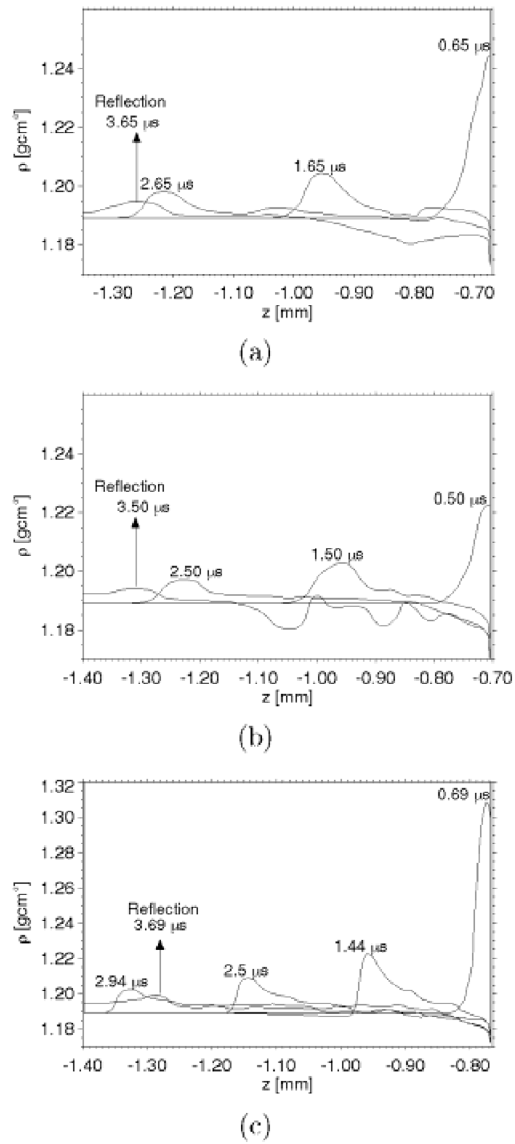

Fig. 4. Density profiles at different times in plexiglass, after the beam was stopped in the absorber material: (a) Cu, (b) Fe, and (c) Pb. At later times, the reflected wave on the interface between the plexiglass layer and the Al witness layer is observed.

5. CONCLUSIONS

The behavior of the weak shock waves induced by the heavy ion beam inside solid targets was studied for the first time, space and time resolved, with a schlieren technique. A spherical, thick shock front with pressures of up to 15 kbar and with a strength declining in time was observed over some tens of microseconds as the pictures recorded at later times (up to 30 μs delay) showed. The shock propagation velocities in the plexiglass layer were up to 1.35 times higher than

https://doi.org/10.1017/S0263034602202281 Published online by Cambridge University Press

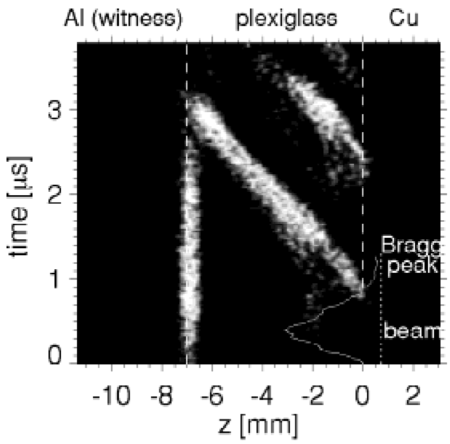

(a)

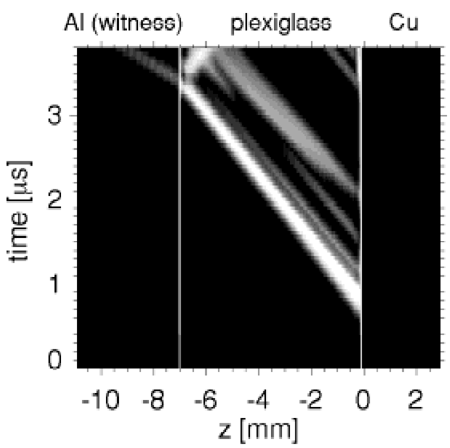

(b)

Fig. 5. Experimental (a) and simulated (b) streak pictures for a target with a 7-mm-long Cu absorber in front of the plexiglass layer.

the speed of sound at room temperature, for a simulated temperature increase of less than 4 K. The spherical shape of the shock front and the thickness of the target introduced uncertainties in the calculation of the density gradients created by the shocks in the plexiglass, based on relations (1) and (2) with deflection angles measured experimentally. Therefore, the determination of densities and density gradients was accomplished by using the simulations. A good agreement was found between measured and calculated parameters such as pressures, wave propagation velocity, and velocity of the expanding matter in front of the target and the time history of the multiple pressure waves for the targets with Cu and Pb absorbents. More benchmarks will be provided by upcoming experiments, oriented towards interferometric measurements of the density inside the sample material and, simultaneously, direct measurements of the pressures by using polyvinylidene fluoride (PVDF) pressure gauges implemented in the targets. The geometry and the design of the targets will be changed as well. The plexiglass will be replaced by rare gas and hydrogen cryogenic crystals, while the absorber will be chosen based on an acoustic impedance mismatch in order to shape planar shock fronts, desired for effective measurements. Promising perspectives for the beam parameter upgrade are given by the bunching of the beam pulses down to 50 ns duration (Spiller & Hofmann, 1998) and an intensity increase leading to higher compression ratios and pressures in the megabar range, as asserted by theoretical calculations (Tahir *et al.*, 2000). This is a new regime of high energy density studies, proper for fundamental research in phase transition physics and EOS properties of matter under extreme conditions.

ACKNOWLEDGMENT

This work was supported by the German Federal Ministry of Education and Research (BMBF).

REFERENCES

Aoki, T. & Meyer-ter-Vehn, J. (1994). Dynamic compression of hydrogen for probing the molecular-atomic phase transition. *Phys. Plasmas*. **1**, 1962–1970.

Baumung, K., Bluhm, H.J., Goel, B., Hoppé, P., Karow, H.U., Rusch, D., Fortov, V.E., Kanel, G.I., Razonerov, S.V., Utkin, A.V. & Vorobiev, O.Yu. (1996). Shock-wave physics experiments with high-power proton beams. *Laser Part. Beams* **14**, 181–209.

Bushman, A.V. & Fortov, V. (1987). *Sov. Tech. Rev. B.-Therm. Phys.1* **219**.

Collins, G.W., Da Silva, L.B., Celliers, P., Gold, D.M., Foord, M.E., Wallace, R.J., Ng, A., Weber, S.V., Budil, K.S. & Cauble, R. (1998). Measurements of the equation of state of deuterium at the fluid insulator-metal transition. *Science* **281**, 1178–1181.

Da Silva, L.B., Celliers, P., Collins, G.W., Budil, K.S., Holmes, N.C., Barbee, T.W., Jr., Hammel, B.A., Kilkenny, J.D., Wallace, R.J., Ross, M., Cauble, R., Ng, A. & Chiu, G. (1997). Absolute equation of state measurements on shocked liquid deuterium up to 200 GPa (2 Mbar). *Phys. Rev. Lett.* **78**, 483–486.

Fortov, V.E., Goel, B., Munz, C.-D., Ni, A.L., Shutov, A.V. & Vorobiev, O.Yu. (1996). Numerical simulations of nonstationary fronts and interfaces by the Godunov method in moving grids. *Nucl. Sci. Eng.* **123**, 169–189.

Funk, U.N., Bock, R., Dornik, M., Geissel, M., Stetter, M., Stöwe, S., Tahir, N.A. & Hoffmann, D.H.H. (1998). High energy density in solid rare gas targets and solid hydrogen. *Nucl. Instrum. Methods Phys. Res. A* **415**, 68–74.

Jahoda, F.C. & Sawyer, G.A. (1971). Plasma physics. In *Methods of Experimental Physics* (Lovberg, R.H. and Griem, H.R., Eds.), Vol. 9, Part B. New York: Academic Press.

Lomonosov, I.V., Bushman, A.V. & Fortov, V. (1994). In *High Pressure Science and Technology* (Schmidt, S.C., Schaner, J.W., Samara, G.A. and Ross, M., Eds.), Pt. 1, p. 117. New York: AIP.

Mao, H.K. & Hemley, R.J. (1994). Ultrahigh-pressure transitions in solid hydrogen. *Rev. Mod. Phys.* **66**, 671–692.

Marton, L. & Marton, C. (1981). Fluid dynamics. In *Methods of Experimental Physics* (Emrich, R.J., Ed.), Vol. 18, Part A. New York: Academic Press.

Schlegel, Th., Meyer-ter-Vehn, J., Hoffmann, D.H.H., Ramirez, J. & Ramis, R. (2001). EOS investigations by low entropy compression of matter. *Contrib. Plasma Phys.* **41**, 167–170.

Spiller, P. & Hofmann, I. (1998). Optics of final beam transport and focusing for a heavy-ion ignition facility. *Nucl. Instrum. Methods Phys. Res. A* **415**, 384–388.

Stetter, M., Christiansen, J., Neuner, U., Stoewe, S., Tkotz, R., Wagner, T., Boggasch, E., Tauschwitz, A., Hoffmann, D.H.H. & Spiller, P. (1993). Development of a plasma lens as a fine focusing lens for heavy-ion beams. *Nouvo Cimento A* **106**, 1725–1731.

Stetter, M., Neuner, U., Stoewe, S., Dornik, M., Hoffmann, D.H.H., Kowalewicz, R., Spiller, P. & A. Tauschwitz. (1996). The high current plasma lens: Investigations of the fine focusing of high energy heavy ion beams. *Fusion Eng. Des.* **32–33**, 503–509.

Stöwe, S., Bock, R., Dornik, M., Spiller, P., Stetter, M., Fortov, V.E., Mintsev, V., Kulish, M., Shutov, A., Yakushev, V., Sharkov, B., Golubev, A., Bruynetkin, B., Funk, U.N., Geissel, M., Hoffmann, D.H.H. & Tahir, N.A. (1998). High density plasma physics with heavy-ion beams. *Nucl. Instrum. Methods Phys. Res. A* **415**, 61–67.

T4 Group (1983). *SESAME report on the Los Alamos equation-of-state library*. Report No. LALP-83-4. Los Alamos, NM: Los Alamos National Laboratory.

Tahir, N.A., Hoffmann, D.H.H., Maruhn, J.A., Spiller, P. & Bock, R. (1999). Heavy ion beam induced hydrodynamic effects in solid targets. *Phys. Rev. E* **60**, 4715–4724.

Tahir, N.A., Hoffmann, D.H.H., Kozyreva, A., Shutov, A., Maruhn, J.A., Neuner, U., Tauschwitz, A., Spiller, P. & Bock, R. (2000). Shock compression of condensed matter using intense beams of energetic heavy ion. *Phys. Rev. E* **61**, 1975–1980.

Tahir, N.A, Hoffmann, D.H.H., Kozyreva, A., Tauschwitz, A., Shutov, A., Maruhn, J.A., Spiller, P., Neuner, U., Jacoby, J., Royh, M., Bock, R., Juranek, H. & Redmer, R. (2001). Metallization of hydrogen using heavy-ion beam implosion of multilayered cylindrical targets. *Phys. Rev. E* **63**, Print Issue, 016402 (9 pages).

Weir, S.T., Mitchell, A.C. & Nellis, W.J. (1996). Metallization of fluid molecular hydrogen at 140 GPa (1.4 Mbar). *Phys. Rev. Lett.* **76**, 1860–1863.

Wigner, E. & Huntington, H.B. (1935). On the possibility of a metallic modification of hydrogen. *J. Chem. Phys.* **3**, 764–770.

Zhang, B.-P. & Müller, F. (1984). The dynamic behaviour of poly(methyl metacrylate) in the low-pressure range. *High Temp.-High Press.* **16**, 475–483.

Ziegler, J.F., Biersack, J.P. & Littmark, U. (1996). *The Stopping and Ranges of Ions in Solids*. New York: Pergamon.

https://doi.org/10.1017/S0263034602202281 Published online by Cambridge University Press